



ELSEVIER

Available online at www.sciencedirect.com

SCIENCE @ DIRECT®

Nuclear Instruments and Methods in Physics Research B 229 (2005) 137–143

NIM B
Beam Interactions
with Materials & Atoms

www.elsevier.com/locate/nimb

Study of a 5 MeV electron linac based neutron source

L. Auditore^{a,b,*}, R.C. Barnà^{a,b}, D. De Pasquale^{a,b}, A. Italiano^a,
A. Trifirò^{a,b}, M. Trimarchi^{a,b}

^a INFN-Gruppo Collegato di Messina, I-98166 Messina, Italy

^b Dipartimento di Fisica dell'Università di Messina, I-98166 Messina, Italy

Received 25 June 2004; received in revised form 28 October 2004

Abstract

A compact neutron source, based on a 5 MeV electron linac, has been designed for Neutron Radiography/Boron-Neutron-Capture-Therapy (BNCT) applications. Although a higher electron energy is generally needed to produce an intense neutron beam, in this paper the use of Be and BeD₂ photoneutron targets will be proposed, leading to thermal neutron beams of 8.48×10^7 n/cm²/s/mA and 1.23×10^8 n/cm²/s/mA, respectively. Optimization of the parameters involved in neutron production (e- γ conversion, moderator and reflector performances) has been studied by means of the MCNP-4C2 code.

© 2004 Elsevier B.V. All rights reserved.

PACS: 29.25.Dz; 29.17.+w

Keywords: Photoneutron; Electron linac; Neutron source

1. Introduction

Reactors, ion accelerators and spallation sources have higher neutron flux and are preferred over electron linacs for their applications in scientific investigation. Nevertheless, such efficient neutron sources can hardly find application in

industrial and medical fields because of disadvantages such as large dimensions or problems related to the authorizations needed for maintenance of reactors or radioactive waste materials.

Moreover, neutron production by means of an electron linac can be pulsed, and the flux intensity can be easily modulated by modifying the electron beam parameters.

The main disadvantage of electron linacs used as neutron source is the low neutron production, in particular when low energies are considered (below 10 MeV). Moreover, in this cases, the target choice is strictly limited to few light elements [2].

* Corresponding author. Address: INFN-Gruppo Collegato di Messina, I-98166 Messina, Italy. Tel.: +39 090393654; fax: +39 090395004.

E-mail address: lauditore@unime.it (L. Auditore).

Nevertheless, neutron production can be optimized by choosing the appropriate materials, components and device dimensions, thus obtaining acceptable results, at least as far as BNCT (Boron-Neutron-Capture-Therapy) [12] and Neutron Radiography [13] are concerned.

In our design, the neutron source optimization was performed by using the MCNP-4C2 (Monte-Carlo-*N*-Particle) [1] simulation code in multitasking mode (with PVM, Parallel-Virtual-Machine, software), considering two different neutron targets, beryllium and beryllium deuteride, showing the lowest (γ, n) energy threshold.

The study was carried out by first optimizing the e- γ conversion which provides the photon beam for the (γ, n) reaction, and then optimizing the photoneutron target, reflector and thermalizing material parameters.

Most of the obtained results show a calculation error of about 2%. Larger errors have been obtained in evaluating the neutron energy spectra as indicated in the corresponding plots.

2. Photoneutron production

In this design, neutrons are produced by (γ, n) reaction, after that a photon beam has been obtained from 5 MeV electrons. The separation energy of the last neutron is about 7–10 MeV for intermediate mass systems and 6–7 MeV for heavy nuclei. As a consequence, to produce neutrons from most of elements, an energy higher than 5 MeV would be necessary. But, for few light elements, such as deuterium and beryllium, this energy is enough to produce neutrons. The (γ, n) cross section for these light elements is quite low, approximately 1–2 *mbarns*: therefore the total process, electron-photon-neutron, has a low efficiency.

The neutron yield from a bremsstrahlung beam, supposing a thin (e, γ) converter, can be obtained from the following formula:

$$Y_n = t \frac{N_A}{A} \int_{E_{\gamma,th}}^{E_{\gamma,max}} \sigma_n(E_\gamma) \frac{dY_\gamma(E_\gamma)}{dE_\gamma} dE_\gamma, \quad (1)$$

where t is the target density, N_A the Avogadro's number, $E_{\gamma,th}$ and $E_{\gamma,max}$ the (γ, n) energy thresh-

old and the maximum photon energy, respectively; σ_n is the microscopic cross section for neutron production and

$$\frac{dY_\gamma(E_\gamma)}{dE_\gamma} \quad (2)$$

represents the bremsstrahlung yield.

The integrated cross section can be evaluated by using the cross section sum-rule for absorption of γ rays, but this leads to a divergence between calculated and measured yields, and this is more evident when light nuclei are involved. This is due to an overestimation of the photoneutron cross sections by this rule. The suggested way to make a valid estimation is to use measured parameters of neutron production cross sections.

Two light targets of Be and BeD₂ [7,8] have been considered. Be and D have (γ, n) energy thresholds of 1.66 MeV and 2.2 MeV, respectively. (γ, n) cross section for Be target reaches the maximum value of about 1.5 *mbarns* in the energy range 1.6–5 MeV while the maximum (γ, n) cross section for D target is approximately 2.2 *mbarns* for 5 MeV photon energy.

BeD₂ seems to be a good choice due to the compromise between the low (γ, n) energy threshold of beryllium, and the higher deuterium cross section.

3. The bremsstrahlung converter

Electrons impinging on a target interact with it producing photons, whose energy is distributed according to a continuum spectrum with end point equal to the electron energy.

The energy spectrum of the produced X-rays can be evaluated as [3,10,11]

$$\frac{d^2Y}{dk d\Omega}(T_e, k, \omega) = \sum_{i=1}^n \eta_i(k, d_i, \omega) \tau_i(T_e, d_i) N_i \times \frac{d\sigma}{dk} [(T_e)_i, k] B_i(\omega), \quad (3)$$

which provides the spectrum as Photons/electron/sr/MeV and is calculated by dividing the whole target material thickness in n layers and evaluating the X-ray production and diffusion in each layer.

The terms appearing in Eq. (3) can be estimated as explained in [10,11] and take into account all the parameters influencing the X-rays production, such as target material, electron energy loss, $[(T_e)_i, k]$, electron scattering inside the target material, $B_i(\omega)$, electron transmission coefficient, $\tau_i(T_e, d_i)$, and photon mass attenuation coefficient, $\mu(k)$.

The total bremsstrahlung yield is theoretically expressed by the Bethe–Heitler equation and several approximations allow to solve it for practical calculations. The MCNP-4C2 code uses the Bethe–Heitler Born approximation results for sampling the bremsstrahlung photons while the involved bremsstrahlung cross sections are based upon the evaluations by Berger and Seltzer [4–6,9].

In our design several simulations [14] were carried out to evaluate materials and thicknesses enhancing the bremsstrahlung yield. A 1 MeV energy cut was considered; lower energy photons will not contribute to the neutron production due to the (γ, n) energy thresholds for the two chosen photoneutron targets.

For each material, a plot showing the yield versus the converter thickness was obtained and the bremsstrahlung spectra were simulated for the thickness corresponding to the highest photon yield. Such a study enabled us to choose a tungsten converter, providing the highest photon yield in the 1–5 MeV range. The photon yield versus W thickness plot of Fig. 1 shows a maximum in the 1.5–1.8 g/cm² range. For increasing thicknesses,

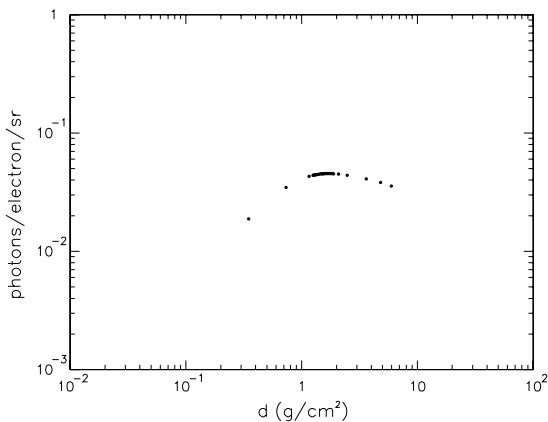


Fig. 1. Photon yield as a function of the W converter thickness.

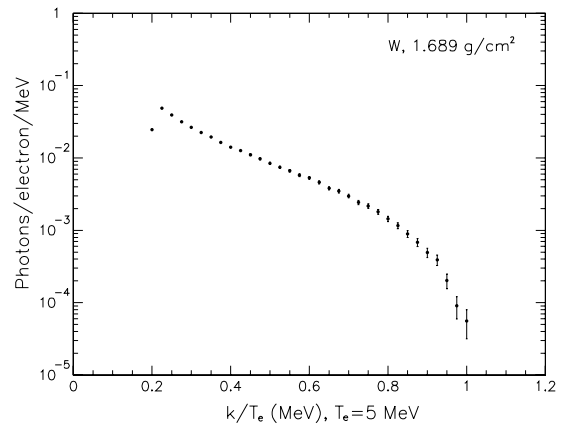


Fig. 2. Bremsstrahlung spectrum for a 1.698 g/cm² thick W converter.

although a greater number of photons is produced, their absorption in the material decreases the total photon emission. Then, the 1.698 g/cm² thickness was chosen for the W converter, which corresponding bremsstrahlung spectrum is shown in Fig. 2. 5 MeV electrons in tungsten have a range larger than the chosen thickness, and we expect about 7% of incident electrons beyond the converter, with an energy lying in the range 1.6–3.6 MeV, consequently they could enter the photoneutron target and produce further photons with energy higher than 2 MeV, then contributing to the neutron production.

4. Photoneutron target optimization

4.1. Target and reflector parameters

The cylindrical shape has been chosen for the photoneutron target, being the easier one to carry out.

Dimensions were estimated at first by simulating the angular distribution of photons coming from the converter, and then calculating the photoneutron target thickness in which a bremsstrahlung photon would have interacted producing a neutron.

The beryllium deuteride target was designed as a beryllium deuteride core surrounded by a 4cm-thick beryllium layer, see Fig. 4. This configuration

would enhance the probability for low energy photons to produce neutron in the outer target shell.

Both targets were surrounded by a reflector reducing the neutron losses from the photoneutron target walls. Moreover, a conic-shaped reflector was inserted beyond the photoneutron target.

The scheme of the final neutron source is shown in Figs. 3 and 4 for Be and BeD₂ sources, respectively.

Graphite was chosen as the reflecting material and its thickness was set at 50 cm, a good compromise between the need to design a compact source and to reflect as many neutron as possible toward the forward direction. In Fig. 5 neutron flux versus distance from the photoneutron target is shown. It can be seen that for graphite thicknesses greater than 40 cm the neutron flux inside the conic-shaped reflector reaches a maximum value. Similar

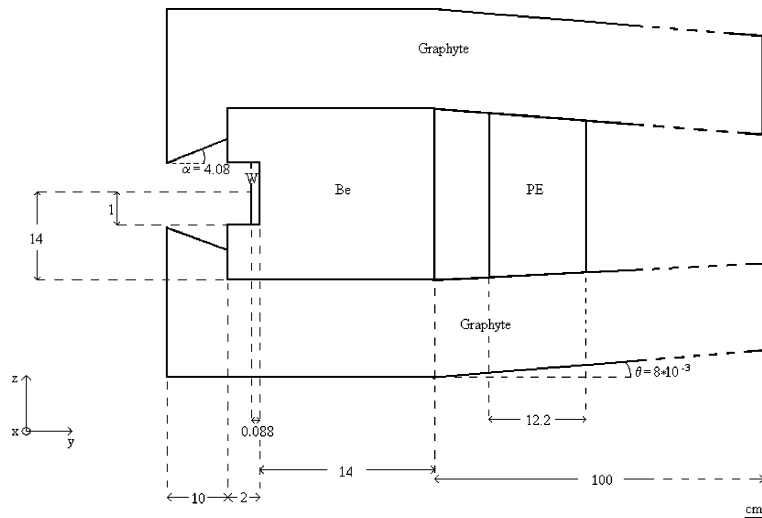


Fig. 3. Scheme of the Be-based neutron source.

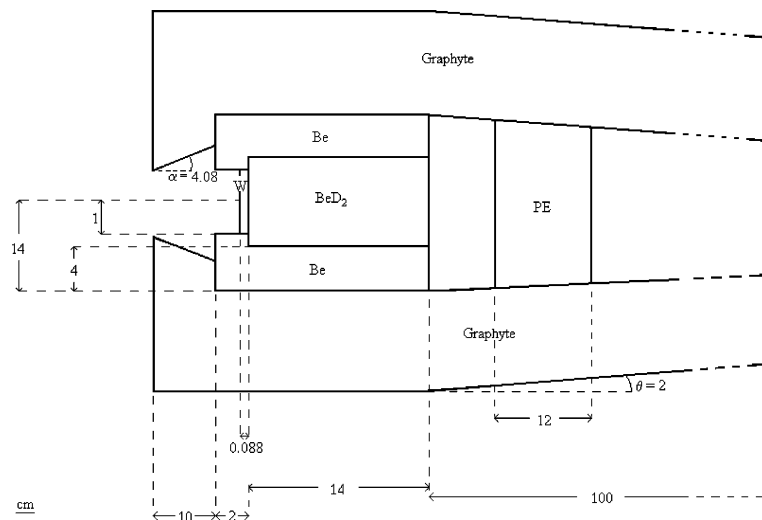


Fig. 4. Scheme of the BeD₂-based neutron source.

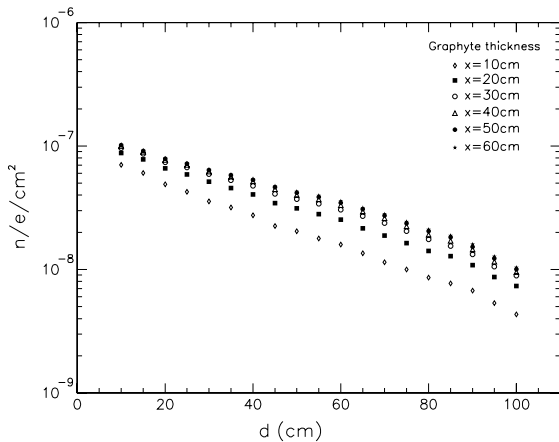


Fig. 5. Neutron flux dependence on graphite thickness.

results were obtained for the beryllium deuteride target. Lead was also considered as a possible reflector, thus providing a shielding of photons not absorbed by the target. However, lead is less reflecting than graphite, thus giving rise to a less intense neutron beam if compared with the one obtained with the graphite reflector.

4.2. Neutron thermalization

The possible applications of the neutron beam plays an important role to determine the final neutron energy. Neutron fluxes of 6.25×10^{-8} ($\pm 2\%$) $n/e/cm^2$ and 9.33×10^{-8} ($\pm 2\%$) $n/e/cm^2$, showing a continuous energy spectrum up to about 2 MeV, have been obtained from beryllium and beryllium deuteride respectively. If compared with neutron beams from ion accelerators or reactors, this beam could appear not intense but enough to be employed in industrial and medical fields, if thermalized.

Good moderators should provide a high *average logarithmic energy decrement* ξ value, then requiring few collisions to thermalize neutrons, and reducing the probability that they are absorbed along their path inside the moderator. Such moderators should then provide a short *diffusion length*, L , which represents the average shortest point-to-point distance from the source which neutrons reach before absorption.

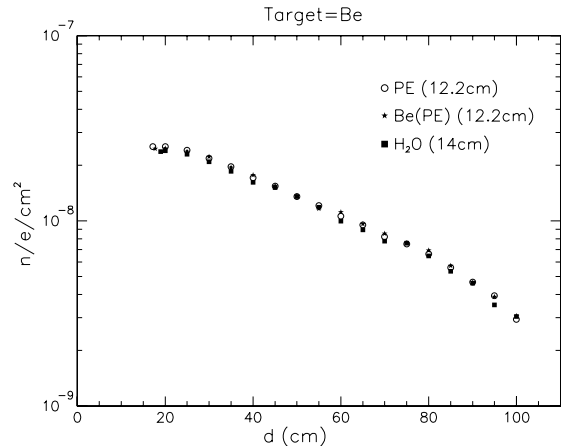


Fig. 6. Neutron fluxes from PE, Be(PE) and H₂O moderators for Be target.

The most moderating materials are polyethylene (PE), water (H₂O) and heavy water (D₂O). ¹⁰Be loaded PE was also considered. D₂O was rejected due to the thickness (about 100 cm) needed to thermalize neutrons.

A comparison among different moderators is shown in Fig. 6 for Be target.

The considered moderators are all equivalent in thermalizing and absorbing neutrons. Then, a 12.2 cm and 12 cm polyethylene slab were chosen as the final moderators for Be and BeD₂ targets, respectively. The difference in moderator thicknesses is due to the mean energy of fast neutrons

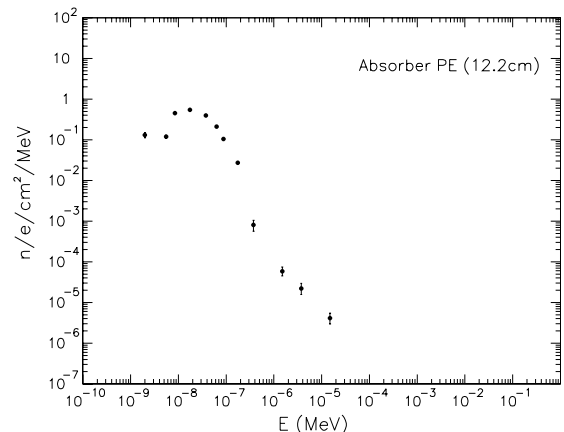


Fig. 7. Neutron energy spectrum from the Be-based source, at 50 cm from the target.

coming from the two photoneutron targets. Neutrons from Be show a mean energy higher than the one provided by neutrons from BeD₂ thus requiring a higher number of collisions (then a thicker moderator) to be slowed down to the thermal energy of 25 meV.

A thermal neutron flux of 8.48×10^7 n/cm²/mA/s from Be and of 1.23×10^8 n/cm²/mA/s from BeD₂ was obtained. In Figs. 7 and 8 the neutron energy spectra for the two considered targets are shown: clearly they show a maximum around 25–30 meV. Plotted data are limited to energy values

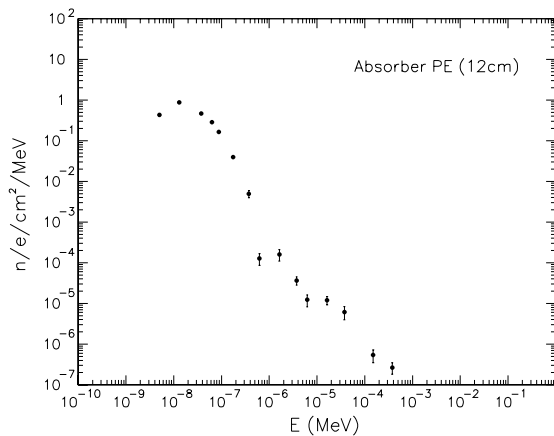


Fig. 8. Neutron energy spectrum from the BeD₂-based source, at 50cm from the target.

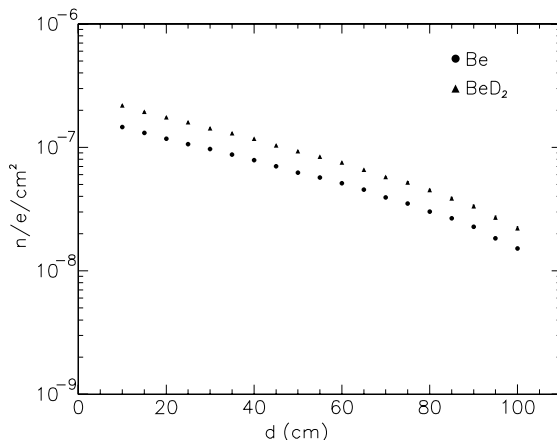


Fig. 9. Comparison between neutron beam intensities obtained with Be and BeD₂ targets.

around 10^{-4} – 10^{-3} MeV due to the more decreasing statistics and the corresponding decrease in calculation precision, which influences the reliability of the obtained data. Comparing the results from the two different photoneutron targets, (see Fig. 9), BeD₂ provide a neutron flux 1.4–1.5 times more intense than the neutron beam from Be.

5. Conclusions

The study of a neutron source based on a low energy electron linac was performed. Beryllium and beryllium deuteride targets were considered. A neutron beam of 8.48×10^7 n/s/cm²/mA at a 50 cm distance from the target was obtained from the Be target and a 1.5 times more intense beam was obtained from the BeD₂ target.

The studied neutron source can be regarded as a further application of the 5 MeV electron linac of the Dipartimento di Fisica, Università di Messina [15]. The simple technology and the limited dimensions of this linac seem to be a good starting point to carry out the studied source providing a good neutron flux, since compactness and simplicity of the device are the main features of this neutron source.

Acknowledgements

Thanks are due to Dr. L. Petrizzi, Sez. Tecnologie e Fusione, ENEA, Frascati, for his collaboration to this project.

The authors thank the staffs of the Computational Center of the ENEA of Frascati and of the Centro di Calcolo ‘A. Villari’, Università di Messina, on which workstations all the simulations were performed.

The authors wish to thank also Dr. Zane W. Bell, BWXT-Y12, L.L.C., Oak Ridge, TN, USA, for his useful indications.

References

- [1] MCNP4C2, By Diagnostics Applications Group, Los Alamos National Laboratory, Los Alamos, New Mexico, USA and Radiation Safety Information Computational

- Center Oak Ridge National Laboratory, Oak Ridge, TN, USA.
- [2] V.L. Chakhlov, Z.W. Bell, V.M. Golovkov, M.M. Shtein, *Nucl. Instr. and Meth. A* 422 (1999) 5.
 - [3] H.W. Koch, J.W. Motz, *Rev. Mod. Phys.* 31 (1959) 920.
 - [4] S.M. Seltzer, in: M.T. Jenkins, W.R. Nelson, A. Rindi (Eds.), *Monte Carlo Transport of Electrons and Photons*, Plenum Press, New York, 1988, p. 81.
 - [5] S.M. Seltzer, M.J. Berger, *Nucl. Instr. and Meth. B* 12 (1985) 95.
 - [6] S.M. Seltzer, M.J. Berger, *Atom. Data Nucl. Data Tables* 35 (1986) 345.
 - [7] N.A. Chirin, V.M. Dorogotovtsev, V.V. Gorlevsky, O.N. Krokhin, Yu.E. Markushkin, Yu.A. Merkul'ev, S.A. Startsev, A.K. Shikov, A.V. Zabrodin, *Proceedings SPIE*, Vol. 4424, ECLIM 2000, Prague, p. 159.
 - [8] N.G. Borisenko, V.M. Dorogotovtsev, A.I. Gromov, S. Yu. Guskov, Yu.A. Merkul'ev, Yu.E. Markushkin, N.A. Chirin, A.K. Shikov, V.F. Patrulin, *Fus. Technol.* 38 (2000) 161.
 - [9] IAEA Photoneutron Data, Evaluations by Los Alamos National Laboratory for MCNP or MCNPX Monte Carlo codes.
 - [10] H. Ferdinande, G. Knuyt, R. Van De Vijver, R. Jacobs, *Nucl. Instr. and Meth.* 91 (1971) 135.
 - [11] Ph.G. Kondev, A.P. Tonchev, Kh.G. Khristov, V.E. Zhuchko, *Nucl. Instr. and Meth. B* 71 (1992) 126.
 - [12] S. Green, *Rad. Phys. Chem.* 51 (1998) 561.
 - [13] E.H. Lehmann, Neutron imaging, in: *Proceedings of 18th Summer School on Neutron Scattering*, Zuoz, August 2000, Publ. World Scientific Publishing Co. Ltd., ISBN 981-02-4444-4.
 - [14] L. Auditore, Study of a Photoneutron Source based on a 5 MeV Electron Linac, Ph.D. thesis 2004, unpublished.
 - [15] L. Auditore, R.C. Barnà, D. De Pasquale, A. Italiano, A. Trifirò, M. Trimarchi, *Phys. Rev. ST* 7 (2004) 030101.